Materials Science & Engineering A 692 (2017) 67–74

Contents lists available at ScienceDirect

Materials Science & Engineering A

journal homepage: www.elsevier.com/locate/msea

The effects of thin coatings on the mechanical properties and resistance to annealing-induced embrittlement of bulk metallic glass

Z.Q. Chen[a], L. Huang[a], P. Huang[a,*], K.W. Xu[a], F. Wang[b,*], T.J. Lu[b,c]

[a] State Key Laboratory for Mechanical Behavior of Material, Xi'an Jiaotong University, Xi'an 710049, China
[b] State Key Laboratory for Strength and Vibration of Mechanical Structures, Xi'an Jiaotong University, Xi'an 710049, China
[c] MOE Key Laboratory for Multifunctional Materials and Structures, Xi'an Jiaotong University, Xi'an 710049, China

ARTICLE INFO

Keywords:
Bulk metallic glass
Coating
Plasticity
Strength
Embrittlement

ABSTRACT

The effect of thin coating on the strength, plasticity and resistance to annealing-induced embrittlement was investigated for $Zr_{50.7}Cu_{28}Ni_9Al_{12.3}$ bulk metallic glass (BMG). To maintain the BMG structure in the most extent, very thin amorphous CuZr and crystalline W coatings were used. The crystalline coating performed much better in improving BMG plastic deformation than the amorphous one, for its superior retarding effect on shear band (SB) dynamics. Besides the coatings, softer layers near the sputtered surfaces also contributed to the enhanced plasticity of the coated BMG. The presence of these softer layers also led to the slightly lower strength of both amorphous CuZr and crystalline W coated BMGs relative to the uncoated ones. The BMG with crystalline W coating exhibited much better resistance to annealing-induced embrittlement than the amorphous CuZr-coated and uncoated ones, due to its much enhanced decomposition processes upon annealing. These experimental results provide useful guidance on choosing suitable coating materials to elevate BMG plasticity and avoid annealing-induced embrittlement.

1. Introduction

The inherent brittleness of bulk metallic glasses (BMGs), manifested as catastrophic fracture with deformation localized into a main narrow shear band (SB), severely limits their practical application as a structural material [1,2]. Even worse, annealing-induced embrittlement in BMGs due to running off of free volume (FV) [3,4] may further restrict their application in the environment of elevated temperature.

To improve the plasticity of BMGs, many kinds of soft crystalline coatings, such as Cu and Ni films, have been used to confine the unstable development of SBs so as to produce more homogeneously distributed SBs [5–10]. However, the soft coatings were about dozens to hundreds of micrometer thick, which distinctly altered the BMGs into BMG/crystal composites. Meanwhile, these soft coatings led to obvious reduction in yield strength of the coated BMGs, as they also participated in deformation besides the BMGs. To avoid this, a hard amorphous NiP coating was used to elevate the plasticity of BMG without obvious sacrifice of its strength [11]. The results indicated that amorphous coatings might be more suitable than crystalline coatings for improving the mechanical properties of BMG.

Concerning the amorphous structure, however, a crystalline coating might be more thermodynamically incompatible with structural defects, for during the exothermic process of grain boundary (GB) relaxation in nanocrystalline alloys, defects like dislocations or voids in the crystalline matrix would annihilate in the GBs with amorphous structure [12–15]. In addition, the FV tends to annihilate at the free surface of MGs [16–18]. Accordingly, the crystalline coating might be more suitable than the amorphous one to prevent the running off of FV in BMGs upon annealing and hence elevate the resistance of BMGs to annealing-induced embrittlement.

This study attempted to evaluate experimentally the effects of thin coatings on the overall performance (e.g., strength, plasticity and resistance to annealing-induced embrittlement) of BMGs. To maintain the BMG structure in the most extent and avoid obvious reduction in yield strength of the coated BMGs, very thin amorphous CuZr and crystalline W coatings were used. The experimental results demonstrated that crystalline coatings could greatly improve both the plasticity and the resistance to annealing-induced embrittlement of BMGs, while amorphous coatings could only mildly improve the plasticity but not the resistance to annealing-induced embrittlement. Both the amorphous CuZr and crystalline W coated BMGs exhibited slightly lower strength than the uncoated ones.

* Corresponding authors.
E-mail addresses: huangping@mail.xjtu.edu.cn (P. Huang), wangfei@mail.xjtu.edu.cn (F. Wang).

http://dx.doi.org/10.1016/j.msea.2017.03.049
Received 25 October 2016; Received in revised form 10 March 2017; Accepted 12 March 2017
Available online 15 March 2017

2. Experimental methods

Zr-based BMG ($Zr_{50.7}Cu_{28}Ni_9Al_{12.3}$) ingots were prepared by arc melting the mixture of high-purity (above 99.9%) metal compositions in a Ti-gettered argon atmosphere. Rectangular plates with dimensions of 35 mm×10 mm×2.0 mm were cut from 40 mm×35 mm×2.0 mm dimensional ingots. The two surfaces with a maximum in-plane area of 35 mm×10 mm of selected plates were mechanically grinded, polished to a mirror finish (The final dimensions of the plates were 35 mm×10 mm×1.5 mm), and then coated with amorphous $Cu_{50}Zr_{50}$ (or crystalline W) thin films (~100 nm in thickness) via magnetron sputtering to form sandwich samples. Subsequently, both the as-cast and the coated BMGs were annealed at 573 K for 3 h in a vacuum furnace (~10^{-5} Pa) and eventually cooled down to room temperature in vacuum for more than 24 h. Thence, the six different kinds of samples, i.e., as-cast BMG, annealed BMG, as-deposited CuZr-coated BMG, annealed CuZr-coated BMG, as-deposited W-coated BMG and annealed W-coated BMG samples were termed hereafter as $BMG_{as\text{-}cast}$, $BMG_{annealed}$, $CuZr/BMG/CuZr_{as\text{-}deposited}$, $CuZr/BMG/CuZr_{annealed}$, $W/BMG/W_{as\text{-}deposited}$ and $W/BMG/W_{annealed}$, respectively.

The microstructure of each sample was characterized with X-ray diffraction (XRD-7000Shimadzu Corporation) and transmission electron microscopy (TEM, JEOL JEM-2100F). The energy disperse spectroscopy (EDS) equipped in the TEM was used to verify the composition of the samples. For each sample, the rectangular plate was cut into small compression specimens with identical dimensions of 1.5 mm×1.5 mm×3.0 mm. For each compression specimen, the lateral surfaces (except for the coated ones) were grinded and then polished using waterproof abrasive paper. Quasi-static uniaxial compression tests were conducted on a computer-controlled testing machine (SUNS CMT 5105) at room temperature, with a constant strain rate of 5.6×10^{-4} s^{-1}. At least three specimens were tested for each sample to ensure the reliability of experimental results. After each test, scanning electron microscopy (SEM, SU6600) was used to examine the fracture surface.

3. Results and discussion

The amorphous nature of $BMG_{as\text{-}cast}$, $BMG_{annealed}$, $CuZr/BMG/CuZr_{as\text{-}deposited}$ and $CuZr/BMG/CuZr_{annealed}$, as well as BMGs in $W/BMG/W_{as\text{-}deposited}$ and $W/BMG/W_{annealed}$ were verified by the XRD results shown in Fig. 1. Due to surface coating, the peak position of amorphous hump in the XRD pattern for these BMG samples had shifted, and the induced shifts were somewhat different between samples having amorphous CuZr and crystalline W coatings. No obvious difference could be observed in the XRD patterns between

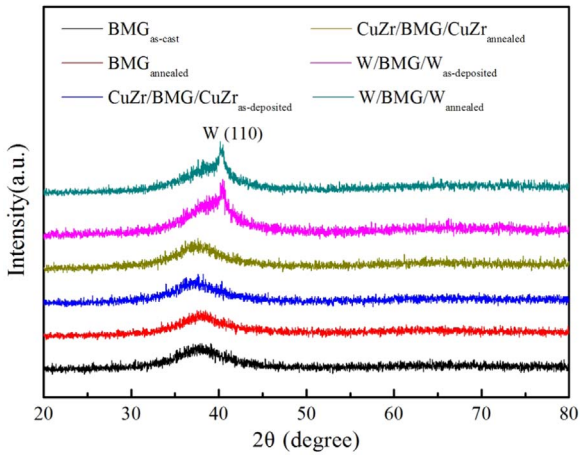

Fig. 1. XRD patterns of coated and uncoated BMG samples before and after annealing treatment.

$BMG_{as\text{-}cast}$ and $BMG_{annealed}$, $CuZr/BMG/CuZr_{as\text{-}deposited}$ and $CuZr/BMG/CuZr_{annealed}$, as well as $W/BMG/W_{as\text{-}deposited}$ and $W/BMG/W_{annealed}$, which indicated that amorphous structures were maintained in all the coated and uncoated BMG samples after annealing treatment.

Fig. 2 displayed the cross-sectional TEM images of amorphous CuZr coatings for $CuZr/BMG/CuZr_{as\text{-}deposited}$ and $CuZr/BMG/CuZr_{annealed}$, as well as crystalline W coatings for $W/BMG/W_{as\text{-}deposited}$ and $W/BMG/W_{annealed}$. No obvious difference could be observed between $CuZr/BMG/CuZr_{annealed}$ [Fig. 2(b)] and $CuZr/BMG/CuZr_{as\text{-}deposited}$ [Fig. 2(a)]. In contrast, compared to $W/BMG/W_{as\text{-}deposited}$ shown in Fig. 2(c), though no other obvious difference could be detected, detachment between crystalline W coating and BMG was observed in $W/BMG/W_{annealed}$ as indicated by the yellow arrow in Fig. 2(d). This should be induced by the mismatch of thermal expansion between the coating and the BMG [19].

Cross-sectional TEM images shown in Fig. 3 revealed the internal structure of each sample. In the presence of both amorphous CuZr and crystalline W coatings, the internal structure of the BMG sample remained almost unchanged, as similarly homogeneous structures were observed in $BMG_{as\text{-}cast}$ [Fig. 3(a)], $CuZr/BMG/CuZr_{as\text{-}deposited}$ [Fig. 3(b)] and $W/BMG/W_{as\text{-}deposited}$ [Fig. 3(c)]. Nonetheless, different extents of inhomogeneous structures were observed in these samples after annealing treatment. Particularly, $BMG_{annealed}$ [Fig. 3(d)] possessed the least inhomogeneous structure, in which tiny dark clusters (about several nanometers in diameter) were sparsely distributed, while $CuZr/BMG/CuZr_{annealed}$ [Fig. 3(e)] possessed slightly more inhomogeneous structure with sparsely distributed dark clusters (slightly larger, about a dozen nanometers in diameter). In sharp contrast, the most inhomogeneous structure was observed in $W/BMG/W_{annealed}$ [Fig. 3(f)], in which much larger dark clusters (about dozens of nanometers in diameter) were densely distributed. Note that the internal amorphous nature of the six samples was verified by the inset area diffraction (SAD) images, as no crystalline spot was observed in them, as well as the high resolution TEM (HRTEM) images. For typical instance, with reference to Fig. 3(f), the inset HRTEM image of the dark cluster as indicated by the rectangle exhibited no crystalline phase.

The contrast fluctuations in Fig. 3(d)–(f) could be attributed to elemental fluctuations. To explore this, EDS scanning was performed on 12 randomly selected points in Fig. 3(f): the yellow points 1–6 were located in the dark clusters while the blue points 7–12 were located in the bright regions. Relatively speaking, according to the results summarized in Table 1, the dark clusters were Cu-rich and the bright regions were Zr-rich. This indicated that, upon annealing, decomposition processes, i.e., formation of nano-scaled Zr- and Cu-rich regions, happened in all the coated and uncoated BMG samples. The result was in accord with many previous works [20–25], which showed that Zr-Cu based MGs had a strong tendency to decompose into Zr- and other element (e.g., Cu)-rich regions, since the decomposed state was more stable than the uniformly distributed state for Zr–Cu based MGs (i.e., the decomposition processes happened mainly due to the thermodynamic driving force to lower the system's Gibbs free energy). Furthermore, the decomposition processes were slightly enhanced by the amorphous CuZr coating, while significantly enhanced by the crystalline W coating. As the internal FV would run off from the uncoated BMG upon annealing [3,4] and FV might be a necessary condition for atom transport [26–28], the decomposition process in uncoated BMG should be suppressed by the running off of FV, resulting in the slightly inhomogeneous structure of $BMG_{annealed}$ [Fig. 3(d)].

In comparison, for the W-coated BMG, the crystalline coating could effectively inhibit the running off of FV from the BMG upon annealing [29], and the maintained FV would persistently contribute to atom transport, thus leading to the significant decomposition state in $W/BMG/W_{annealed}$ [Fig. 3(f)]. Besides, the persistent thermal stress in the W-coated BMG during annealing due to distinct thermal expansion mismatch between crystalline W and BMG [19] might also contribute

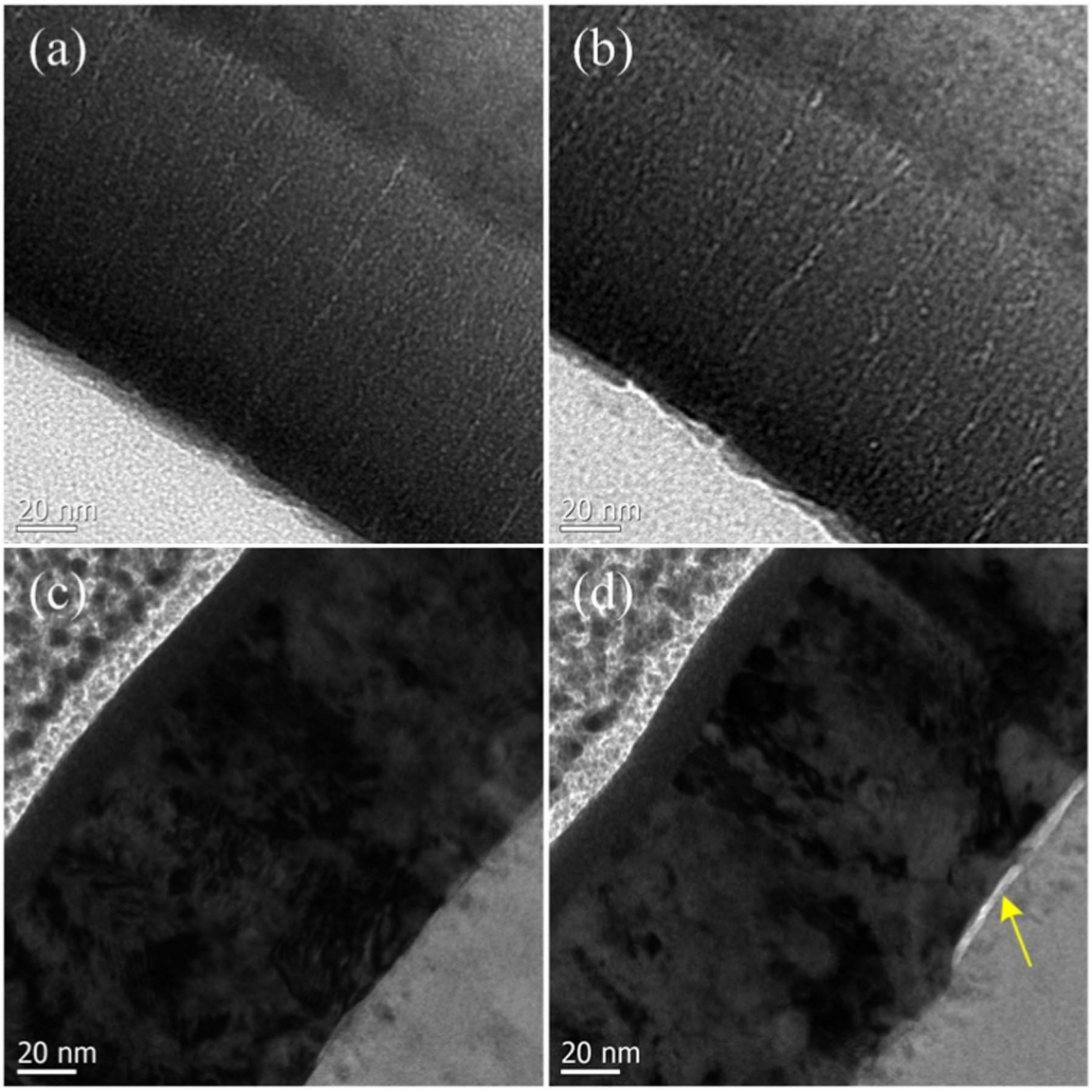

Fig. 2. Cross-sectional bright field TEM images of amorphous CuZr coating in (a) CuZr/BMG/$CuZr_{as\text{-}deposited}$ and (b) CuZr/BMG/$CuZr_{annealed}$, as well as crystalline W coating in (c) W/BMG/$W_{as\text{-}deposited}$ and (d) W/BMG/$W_{annealed}$. Yellow arrow indicated detachment between W coating and BMG. (For interpretation of the references to color in this figure legend, the reader is referred to the web version of this article.)

to the decomposition processes. Relative to crystalline W coating, the amorphous CuZr coating might only delay but not inhibit the running off of FV from the BMG upon annealing, and the thermal expansion mismatch between amorphous CuZr and BMG was minor [19]. Consequently, the decomposition processes in the CuZr-coated BMG were only slightly enhanced relative to the uncoated counterpart, and the structure of CuZr/BMG/$CuZr_{annealed}$ [Fig. 3(e)] was slightly more inhomogeneous than that of $BMG_{annealed}$ [Fig. 3(d)].

Table 2 summarized the room temperature compressive properties of the six kinds of BMG samples, while Fig. 4 plotted their representative compressive uniaxial engineering stress versus strain curves. The BMG samples exhibited similar elastic limit (~2%) but different plastic strains prior to final fracture. Although BMG plasticity was enhanced by both amorphous CuZr and crystalline W coatings, the effect of crystalline W coating was more prominent. Particularly, $BMG_{as\text{-}cast}$ showed a very limited plastic strain of ~0.9 ± 0.1%, followed by abrupt failure, while CuZr/BMG/$CuZr_{as\text{-}deposited}$ showed a mildly increased plastic strain of ~2.6 ± 0.5, also followed by abrupt failure. In sharp contrast, W/BMG/$W_{as\text{-}deposited}$ displayed a greatly enhanced plastic strain of ~6.4 ± 0.7% without abrupt failure, as its plastic deformation during the final stage proceeded with a gradual decreasing stress. Meanwhile, both CuZr/BMG/$CuZr_{as\text{-}deposited}$ and W/BMG/$W_{as\text{-}deposited}$ exhibited a slightly reduced yield strength (~1836 ± 57 and ~1991 ± 53 MPa, respectively), comparing to that (~2027 ± 53 MPa) of $BMG_{as\text{-}cast}$. Moreover, the W-coated BMG had a much better resistance to annealing-induced embrittlement than the uncoated and CuZr-coated BMG samples. For instance, W/BMG/$W_{annealed}$ possessed no reduced plastic strain (6.6 ± 0.1%) relative to W/BMG/$W_{as\text{-}deposited}$, while both $BMG_{annealed}$ and CuZr/BMG/$CuZr_{annealed}$ exhibited only about one half plasticity of the corresponding unannealed samples, with a plastic strain of ~0.5 ± 0.1% and ~1.3 ± 0.3%, respectively. Meanwhile, all the coated and uncoated BMG samples were obviously strengthened after annealing treatment.

For each BMG sample, Fig. 5 presented typical SEM image of its lateral surface morphology near fracture. While sporadic SBs were only observed near the fracture of $BMG_{as\text{-}cast}$ [Fig. 5(a)], apparently more interacted SBs were observed in CuZr/BMG/$CuZr_{as\text{-}deposited}$ [Fig. 5(b)] and the number of SBs further increased and interacted in W/BMG/$W_{as\text{-}deposited}$[Fig. 5(c)]. Relative to unannealed BMG samples, both $BMG_{annealed}$ [Fig. 5(d)] and CuZr/BMG/$CuZr_{annealed}$ [Fig. 5(e)] exhib-

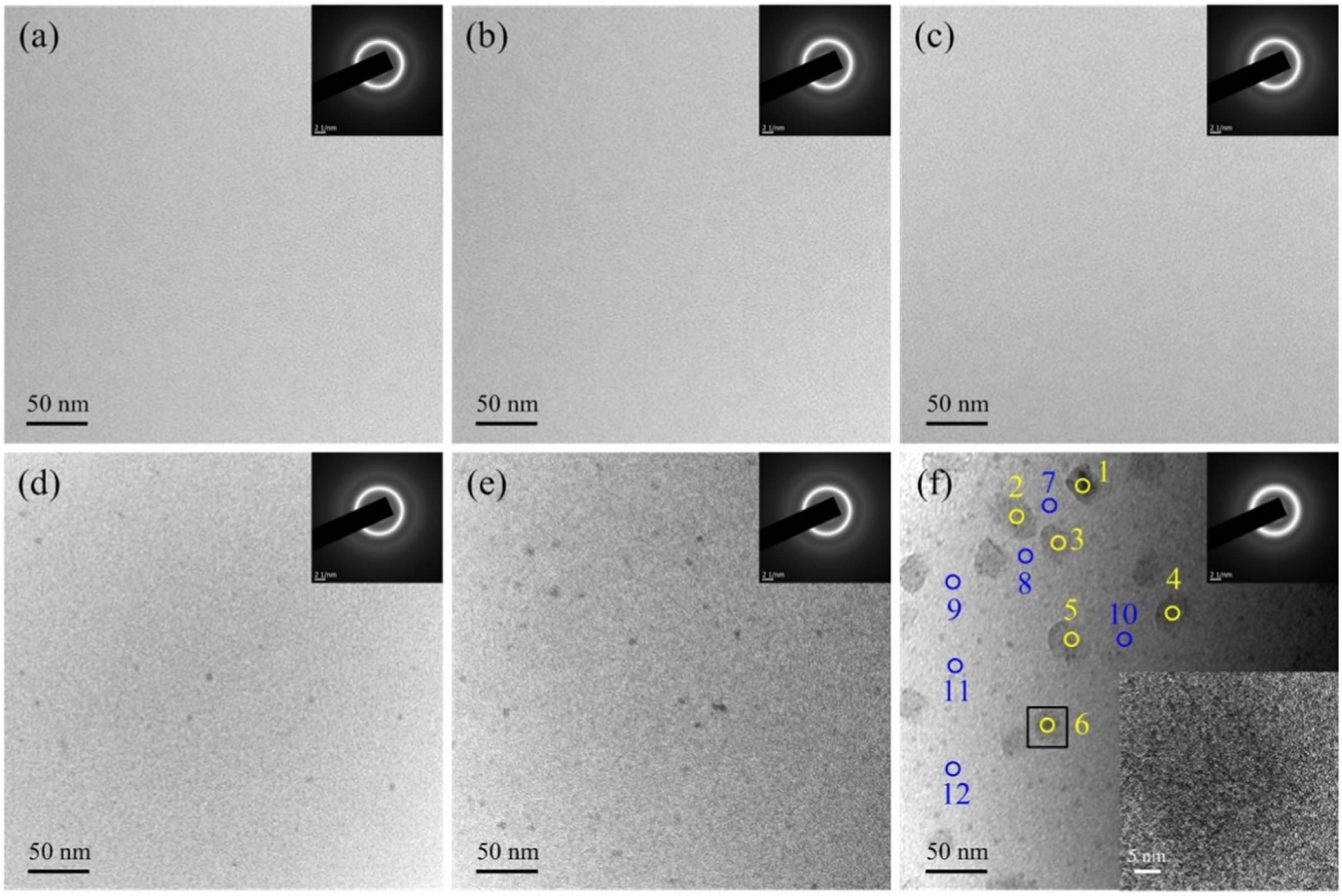

Fig. 3. Cross-sectional bright field TEM images of internal structures in (a) $BMG_{as\text{-}cast}$, (b) $CuZr/BMG/CuZr_{as\text{-}deposited}$, (c) $W/BMG/W_{as\text{-}deposited}$, (d) $BMG_{annealed}$, (e) $CuZr/BMG/CuZr_{annealed}$ and (f) $W/BMG/W_{annealed}$, insert with SAD images. The insert HRTEM image in (d) corresponded to the region indicated by rectangle. (For interpretation of the references to color in this figure, the reader is referred to the web version of this article.)

Table 1
EDS results of scanning randomly selected spots: points 1–6 were located in dark clusters and points 7–12 were located in relatively bright regions.

Spectrum	Element (at%)			
	Zr	Cu	Ni	Al
1	35.28	43.27	9.36	12.09
2	37.47	40.94	9.11	12.48
3	38.35	40.6	8.98	12.07
4	36.27	42.93	8.89	11.91
5	37.93	41.18	9.23	11.66
6	39.04	39.83	9.09	12.04
7	54.58	24.02	9.86	11.54
8	54.08	24.73	9.33	11.86
9	55.62	23.24	9.39	11.75
10	55.76	23.31	8.92	12.01
11	56.53	22.15	9.04	12.28
12	55.41	23.51	8.95	12.13

Table 2
Compressive properties of coated and uncoated BMG samples.

Sample	Yielding strength (MPa)	Plastic strain (%)
$BMG_{as\text{-}cast}$	2027 ± 53	0.9 ± 0.1
$BMG_{annealed}$	2183 ± 58	0.5 ± 0.1
$CuZr/BMG/CuZr_{as\text{-}deposited}$	1836 ± 57	2.6 ± 0.5
$CuZr/BMG/CuZr_{annealed}$	2047 ± 40	1.3 ± 0.3
$W/BMG/W_{as\text{-}deposited}$	1991 ± 53	6.4 ± 0.7
$W/BMG/W_{annealed}$	2154 ± 84	6.6 ± 0.1

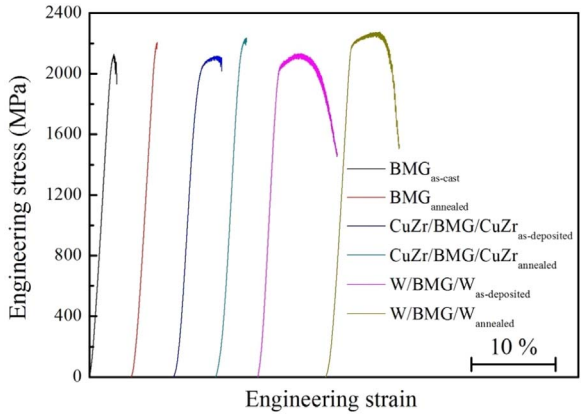

Fig. 4. Representative uniaxial compressive engineering stress versus strain curves of $BMG_{as\text{-}cast}$, $BMG_{annealed}$, $CuZr/BMG/CuZr_{as\text{-}deposited}$, $CuZr/BMG/CuZr_{annealed}$, $W/BMG/W_{as\text{-}deposited}$ and $W/BMG/W_{annealed}$, all tested at room temperature.

ited much reduced SBs, whereas $W/BMG/W_{annealed}$ [Fig. 5(f)] exhibited no reduced but more fine SBs. These results were consistent with existing finding [30] that abundant SBs could sustain plastic deformation cooperatively, rendering good plasticity of BMG. Note that, in accordance with the stress versus strain curves shown in Fig. 4, except for $W/BMG/W_{as\text{-}deposited}$ and $W/BMG/W_{annealed}$, all the other samples failed catastrophically along the dominant shear plane. Especially, due to great brittleness, the fracture of $BMG_{annealed}$ was apparently more cragged than other samples. Meanwhile, in line with their plasticity, the

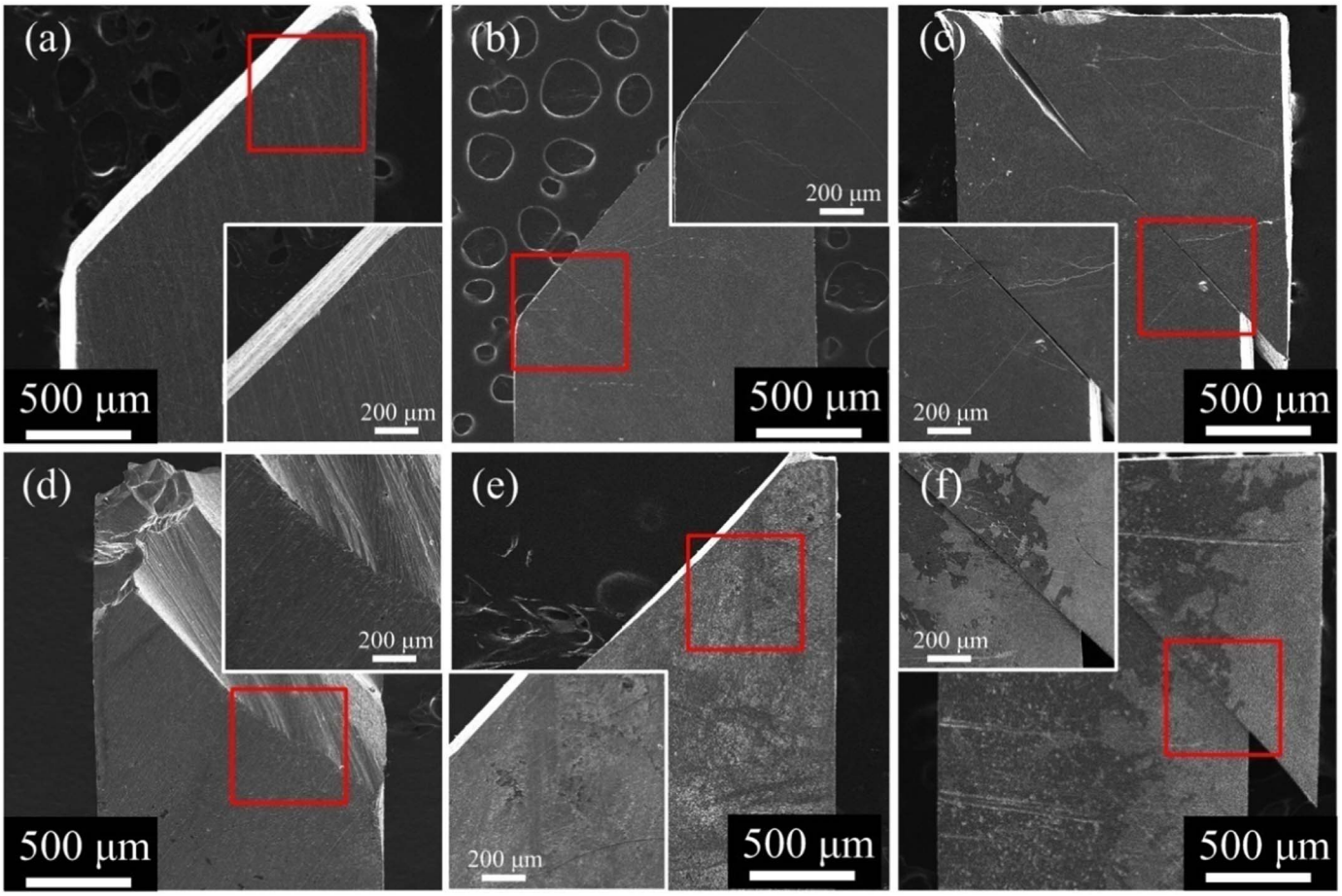

Fig. 5. SEM image of lateral surface morphology of fractured (a) $BMG_{as\text{-}cast}$, (b) $CuZr/BMG/CuZr_{as\text{-}deposited}$, (c) $W/BMG/W_{as\text{-}deposited}$, (d) $BMG_{annealed}$, (e) $CuZr/BMG/CuZr_{annealed}$ and (f) $W/BMG/W_{annealed}$.

fracture surfaces of $W/BMG/W_{as\text{-}deposited}$ [Fig. 6(c)] and $W/BMG/W_{annealed}$ [Fig. 6(f)] exhibited much more vein-like patterns than other samples. In comparison with $CuZr/BMG/CuZr_{as\text{-}deposited}$ [Fig. 6(b)] and $BMG_{as\text{-}cast}$ [Fig. 6(a)], fewer vein-like patterns appeared in $CuZr/BMG/CuZr_{annealed}$[Fig. 6(e)] and $BMG_{annealed}$ [Fig. 6(d)].

High magnification SEM images presented in Fig. 7 revealed that, upon deformation, severe detachment between crystalline W coating and BMG occurred in $W/BMG/W_{annealed}$ [Fig. 7(d)], which agreed with the observation in Fig. 3(d), while only tiny detachment between amorphous CuZr coating and BMG was observed in $CuZr/BMG/CuZr_{annealed}$ [Fig. 7(c)]. In contrast, no such detachments were observed in both deformed $CuZr/BMG/CuZr_{as\text{-}deposited}$ and $W/BMG/W_{as\text{-}deposited}$ [Fig. 7(a) and (b)].

In general, the yielding strength of a coated BMG sample, σ^y, should be estimated using the empirical "rule of mixture", as [31,32]:

$$\sigma^y = \sigma^y_{BMG} f_{BMG} + \sigma^y_c f_c, \quad (1)$$

where σ^y_{BMG} and σ^y_c were the yielding strengths of BMG and coating, respectively, while f_{BMG} and f_c (equal to $1-f_{BMG}$) were the corresponding volume fractions. However, recent studies [5,11] indicated that the "rule of mixture" failed to explain the strength of coated BMGs. For typical instance, in Ren et al.'s study [11], the Vit.1 pillar coated with amorphous NiP, which possessed a higher strength than Vit.1, still showed lower strength than the bare Vit.1 pillar.

In the present study, as both amorphous CuZr and crystalline W coatings possessed a higher strength than the BMG and a very small f_c (~0.013%), the slightly reduced yield strength of $CuZr/BMG/CuZr_{as\text{-}deposited}$ and $W/BMG/W_{as\text{-}deposited}$ should be attributed to some other reasons. Since it had been reported that the sputtering technique, such as shot penning, would induce soft layers near the surface of a BMG [33–35], soft layers might also be induced by magnetic sputtering in the present $CuZr/BMG/CuZr_{as\text{-}deposited}$ and $W/BMG/W_{as\text{-}deposited}$. To explore this, for both coated and uncoated BMGs, hardness data between the area in the middle part and the area near the surface were compared. The results summarized in Table 3 confirmed that soft layers were present near the surface of the coated BMG, although the exact thickness of the soft layers could not be provided. Thence, for the present study, the "rule of mixture" should be revised as:

$$\sigma^y = \sigma^y_{soft} f_{soft} + \sigma^y_{unaffected} f_{unaffected} + \sigma^y_c f_c, \quad (2)$$

where σ^y_{soft} and $\sigma^y_{unaffected}$ were the yielding strength of the soft layer at the surface of sputtered BMG and the unaffected part of the BMG, respectively, and f_{soft} and $f_{unaffected}$ were the corresponding volume fraction. This might explain why the strength of a coated BMG was slightly lower than that of the uncoated one.

On the other hand, the softer layers near the sputtered surfaces of coated BMGs would facilitate SB nucleation during deformation [33–35], thus leading to enhanced plasticity. However, according to the strengths of $CuZr/BMG/CuZr_{as\text{-}deposited}$ and $W/BMG/W_{as\text{-}deposited}$ (Table 2) and the revised "rule of mixture" of Eq. (2), the softer layers in $CuZr/BMG/CuZr_{as\text{-}deposited}$ should be thicker than that in $W/BMG/W_{as\text{-}deposited}$. $W/BMG/W_{as\text{-}deposited}$ showed much better plasticity than $CuZr/BMG/CuZr_{as\text{-}deposited}$, indicating the coatings played a key role in improving the plasticity of BMG. Note that, different from many previous studies [7–9,11,36,37], in which the BMGs were fully-coated with coatings of about dozens to hundreds of micrometers in thickness, the BMGs in the present study were only half-coated with much thinner coatings of ~100 nm in thickness. Consequently, the so called confining

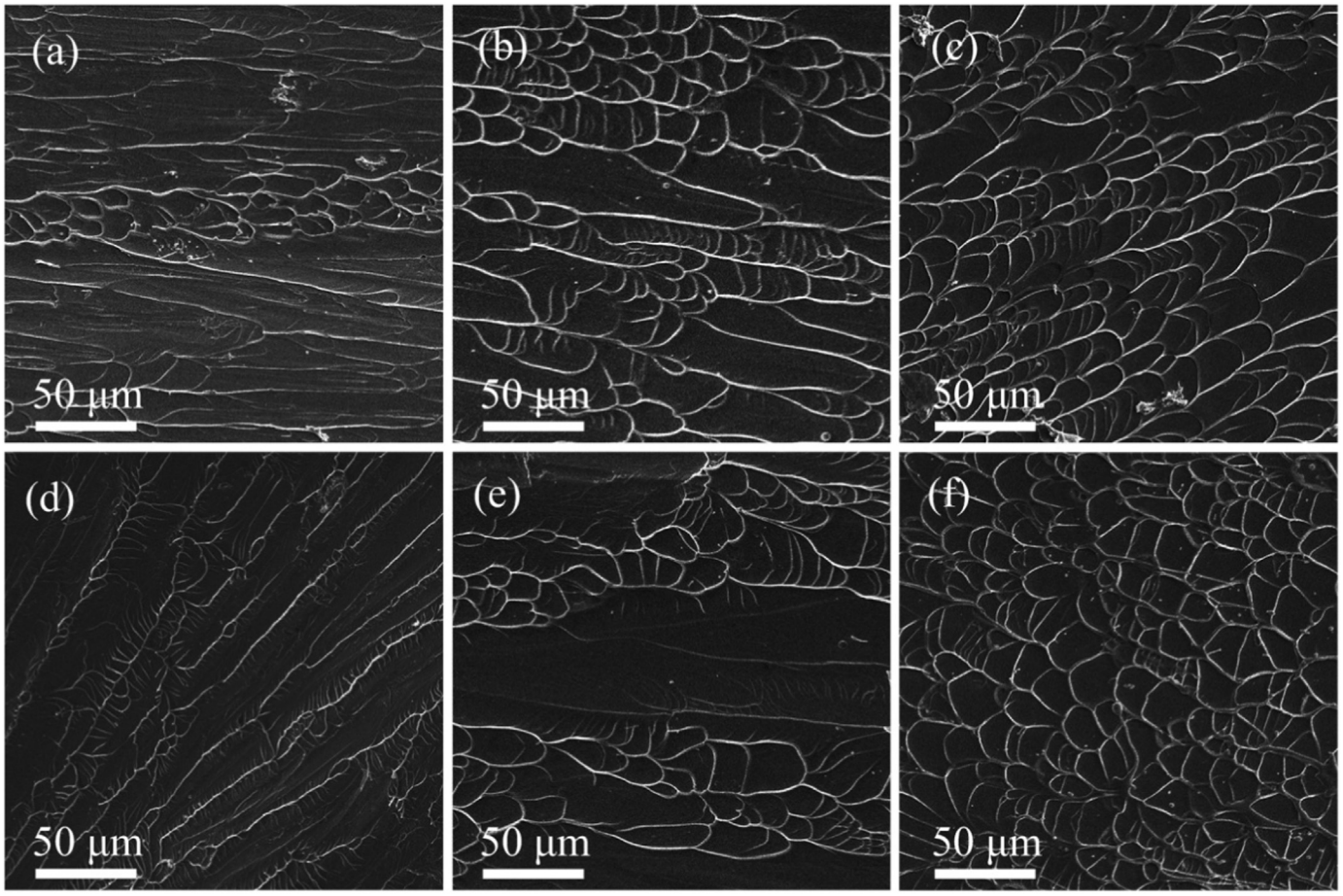

Fig. 6. SEM image of the fractured surface of (a) $BMG_{as\text{-}cast}$, (b) $CuZr/BMG/CuZr_{as\text{-}deposited}$, (c) $W/BMG/W_{as\text{-}deposited}$, (d) $BMG_{annealed}$, (e) $CuZr/BMG/CuZr_{annealed}$ and (f) $W/BMG/W_{annealed}$.

effect [7–9,11,36,37] of coating on bandings deformation in the present BMGs should be much weaker. Actually, a recent study [10] revealed thin coatings could improve BMG plasticity by slowing down SB dynamics to retard its attainment to a critical instable state, termed here as the retarding effect in contrast to the confining effect. Besides, the strength of the coating, as well as the bonding between the coating and BMG, played a key role in contributing to the shear stability of the BMG, since the coating could accommodate the shear banding deformation of BMG by both fracturing and debonding from BMG [10]. However, different from the situation in Ref. [10], where apparent interface debonding happened, no interface debonding could be observed in $W/BMG/W_{as\text{-}deposited}$ and $CuZr/BMG/CuZr_{as\text{-}deposited}$ after compression as shown in Fig. 5(b) and (c), which means that the coating accommodated the shear banding deformation of BMG only by fracturing. Therefore, the strength of the coating should be the main factor that determined the retarding effect of the coating for $W/BMG/W_{as\text{-}deposited}$ and $CuZr/BMG/CuZr_{as\text{-}deposited}$ in this study. As the strength of nanocrystalline W (~3.5 GPa [38]) was much higher than that of amorphous $Cu_{50}Zr_{50}$ (~1.3–1.9 GPa [39]), $W/BMG/W_{as\text{-}deposited}$ would naturally possess a better plasticity than $CuZr/BMG/CuZr_{as\text{-}deposited}$. Furthermore, the more mismatched interface between crystalline W coating and BMG than that between amorphous CuZr coating and BMG would lead to more stress concentrations at the interface, which might also contribute to the better plasticity of $W/BMG/W_{as\text{-}deposited}$ relative to $CuZr/BMG/CuZr_{as\text{-}deposited}$ [8].

Annealing-induced embrittlement and strengthening in uncoated BMG and CuZr-coated BMG samples could be typically explained by the running off of FV during structural relaxation [3,4,40], though mild decomposition processes happened as shown in Fig. 3(d) and (e). However, for the W-coated BMG sample, the annealing-induced embrittlement was suppressed for the significant decomposition state as shown in Fig. 3(f). Relative to the homogeneous amorphous structures in $BMG_{as\text{-}cast}$, $CuZr/BMG/CuZr_{as\text{-}deposited}$ and $W/BMG/W_{as\text{-}deposited}$ [Fig. 3(a), (b) and (c)], as well as the slightly inhomogeneous amorphous structures in $BMG_{annealed}$ and $CuZr/BMG/CuZr_{annealed}$ [Fig. 3(d) and (e)], upon deformation, the larger Zr-rich regions in $W/BMG/W_{annealed}$ (with more local FV) might initiate more easily and serve as flow units to develop into SBs. Meanwhile, the Cu-rich clusters (with less local FV) would hinder the spreading of SBs and hence facilitate the developing of more SBs [41,42]. Besides, similar to second phase in crystalline materials, the stiffer Cu-rich clusters should be responsible for the strengthening of $W/BMG/W_{annealed}$. Note that, since the plasticity of $W/BMG/W_{annealed}$ was comparable to that of $W/BMG/W_{as\text{-}deposited}$ as shown in Table 2, the significant decomposed structure in $W/BMG/W_{annealed}$ made up the deteriorated plasticity due to detachment between crystalline W coating and BMG as shown in Fig. 7(d). After all, such detachment was undesirable and should be avoided. To deal with this issue, more types of coatings would be studied in our further work.

4. Conclusions

It was experimentally demonstrated that the plasticity of BMG could be improved by very thin amorphous CuZr or crystalline W coatings, and the W-coated BMGs exhibited much more plasticity enhancement than the CuZr-coated BMGs. The presence of softer layers near the sputtered surfaces led to slightly lower strength of both the CuZr- and W-coated BMGs than the uncoated ones. While the

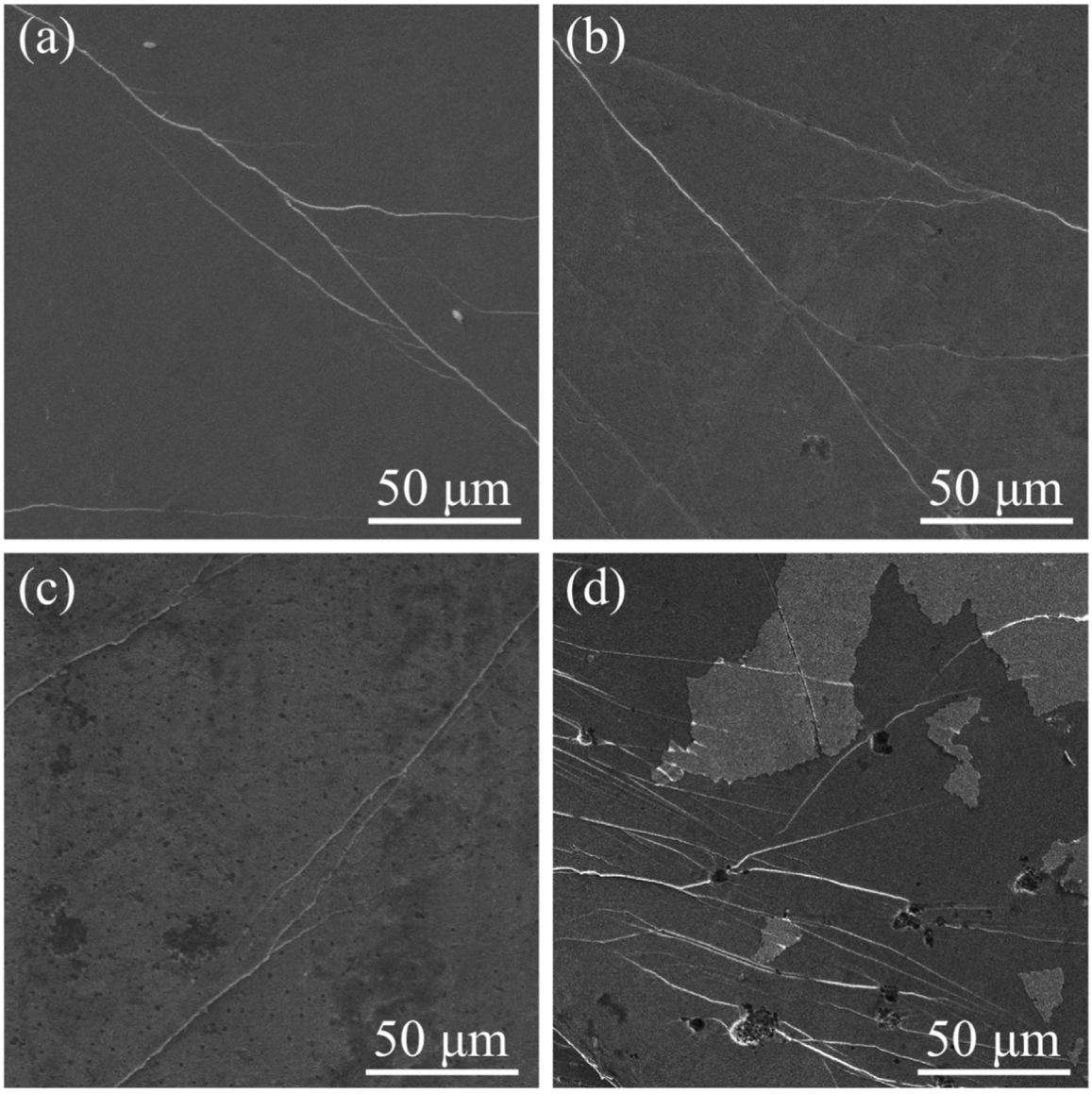

Fig. 7. High magnification SEM images of lateral surface morphology of fractured (a) CuZr/BMG/$CuZr_{as\text{-}deposited}$, (b) W/BMG/$W_{as\text{-}deposited}$, (c) CuZr/BMG/$CuZr_{annealed}$ and (d) W/BMG/$W_{annealed}$.

Table 3
Hardness of the area in the middle part (MP) and the area near the surface (NS; distance from surface ~100 μm) of coated and uncoated BMGs.

Sample		Hardness (GPa)
$BMG_{as\text{-}cast}$	MP	7.65 ± 0.29
	NS	7.66 ± 0.25
CuZr/BMG/$CuZr_{as\text{-}deposited}$	MP	7.55 ± 0.15
	NS	7.04 ± 0.23
W/BMG/$W_{as\text{-}deposited}$	MP	7.68 ± 0.31
	NS	7.19 ± 0.27

softer layers would promote SB nucleation, the coatings had retarding effect on SB developing into a critical instable state during deformation: both mechanisms contributed to BMG plasticity enhancement. As the retarding effect was mainly determined by the strength of the coating in this study, the higher strength of crystalline W coating was mostly responsible for the significantly more plasticity enhancement in W-coated BMGs. Due to the remarkable decomposition processes (formation of Cu-rich clusters and Zr-rich regions upon annealing), the W-coated BMGs exhibited much better resistance to annealing-induced embrittlement than both the CuZr-coated and uncoated BMGs. For the annealed W-coated BMGs, the modified internal structures made up the abated retarding effect of W coating as indicated by the apparent detachment between W coating and BMG upon compression.

Acknowledgements

This work was supported by the National Natural Science Foundation of China (51171141, 51271141 and 51471131).

References

[1] M.M. Trexler, N.N. Thadhani, Mechanical properties of bulk metallic glasses, Prog. Mater. Sci. 55 (2010) 759–839.
[2] C.A. Schuh, T.C. Hufnagel, U. Ramamurty, Mechanical behavior of amorphous alloys, Acta Mater. 55 (2007) 4067–4109.
[3] G. Kumar, D. Rector, R.D. Conner, J. Schroers, Embrittlement of Zr-based bulk metallic glasses, Acta Mater. 57 (2009) 3572–3583.
[4] P. Murali, U. Ramamurty, Embrittlement of a bulk metallic glass due to sub-annealing, Acta Mater. 53 (2005) 1467–1478.
[5] L.W. Ren, M.M. Meng, Z. Wang, F.Q. Yang, H.J. Yang, T. Zhang, J.W. Qiao, Enhancement of plasticity in Zr-based bulk metallic glasses electroplated with

copper coatings, Intermetallics 57 (2015) 121–126.
[6] M. Meng, Z. Gao, L. Ren, H. Yang, S. Ma, Z. Wang, J. Qiao, Improved plasticity of bulk metallic glasses by electrodeposition, Mater. Sci. Eng. A 615 (2014) 240–246.
[7] W. Chen, K.C. Chan, P. Yu, G. Wang, Encapsulated Zr-based bulk metallic glass with large plasticity, Mater. Sci. Eng. A 528 (2011) 2988–2994.
[8] Y.C. Choi, S.I. Hong, Enhancement of plasticity in Zr-base bulk metallic glass by soft metal plating, Scr. Mater. 61 (2009) 481–484.
[9] S.B. Qiu, K.F. Yao, Novel application of the electrodeposition on bulk metallic glasses, Appl. Surf. Sci. 255 (2008) 3454–3458.
[10] B.A. Sun, S.H. Chen, Y.M. Lu, Z.G. Zhu, Y.L. Zhao, Y. Yang, K.C. Chan, C.T. Liu, Origin of shear stability and compressive ductility enhancement of metallic glasses by metal coating, Sci. Rep. 6 (2016) 27852.
[11] L.W. Ren, Z. Wang, M.M. Meng, H. Tian, H.J. Yang, J.W. Qiao, Plasticity enhancement in bulk metallic glasses by electroless plating with Ni-P amorphous films, J. Non-Cryst. Solids 430 (2015) 115–119.
[12] T.J. Rupert, J.R. Trelewicz, C.A. Schuh, Grain boundary relaxation strengthening of nanocrystalline Ni–W alloys, J. Mater. Res. 27 (2012) 1285–1294.
[13] H. Li, F. Jiang, S. Ni, L. Li, G. Sha, X. Liao, S.P. Ringer, H. Choo, P.K. Liaw, A. Misra, Mechanical behaviors of as-deposited and annealed nanostructured Ni–Fe alloys, Scr. Mater. 65 (2011) 1–4.
[14] D. Jang, M. Atzmon, Grain-boundary relaxation and its effect on plasticity in nanocrystalline Fe, J. Appl. Phys. 99 (2006) 083504.
[15] A.J. Detor, C.A. Schuh, Microstructural evolution during the heat treatment of nanocrystalline alloys, J. Mater. Res. 22 (2007) 3233–3248.
[16] L. Shao, E. Fu, L. Price, D. Chen, T. Chen, Y. Wang, G. Xie, D.A. Lucca, Sink property of metallic glass free surfaces, Sci. Rep. 5 (2015) 8877.
[17] C. Nagel, K. Rätzke, E. Schmidtke, F. Faupel, W. Ulfert, Positron-annihilation studies of free-volume changes in the bulk metallic glass $Zr_{65}Al_{7.5}Ni_{10}Cu_{17.5}$ during structural relaxation and at the glass transition, Phys. Rev. B 60 (1999) 9212.
[18] C. Nagel, K. Rätzke, E. Schmidtke, J. Wolff, U. Geyer, F. Faupel, Free-volume changes in the bulk metallic glass $Zr_{46.7}Ti_{8.3}Cu_{7.5}Ni_10Be_27.5$ and the undercooled liquid, Phys. Rev. B 57 (1998) 10224.
[19] H. Kato, H.S. Chen, A. Inoue, Relationship between thermal expansion coefficient and glass transition temperature in metallic glasses, Scr. Mater. 58 (2008) 1106–1109.
[20] R. Busch, E. Bakke, W.L. Johnson, Supercooled melting in multicomponent Zr–Al–Cu–Ni diffusion couples, Appl. Phys. Lett. 68 (1996) 2945–2947.
[21] N. Ismail, M. Uhlemann, A. Gebert, J. Eckert, Hydrogenation and its effect on the crystallisation behaviour of $Zr_{55Cu}30Al_{10}Ni_5$ metallic glass, J. Alloy. Compd. 298 (2000) 146–152.
[22] S.S. Chen, H.R. Zhang, I. Todd, Phase-separation-enhanced plasticity in a $Cu_47.2Zr_{46.5}Al_{5.5N}b_{0.8}$ bulk metallic glass, Scr. Mater. 72–73 (2014) 47–50.
[23] D.H. Kim, W.T. Kim, E.S. Park, N. Mattern, J. Eckert, Phase separation in metallic glasses, Prog. Mater. Sci. 58 (2013) 1103–1172.
[24] E.S. Park, D.H. Kim, Phase separation and enhancement of plasticity in Cu–Zr–Al–Y bulk metallic glasses, Acta Mater. 54 (2006) 2597–2604.
[25] D.V. Louzguine-Luzgin, I. Seki, T. Wada, A. Inoue, Structural relaxation, glass transition, viscous formability, and crystallization of Zr-Cu–based bulk metallic glasses on heating, Metall. Mater. Trans. A 43 (2012) 2642–2648.
[26] D. Turnbull, M.H. Cohen, Concerning reconstructive transformation and formation of glass, J. Chem. Phys. 29 (1958) 1049–1054.
[27] D. Turnbull, M.H. Cohen, Free-volume model of the amorphous phase: glass transition, J. Chem. Phys. 34 (1960) 120–125.
[28] A.V.D. Beukel, J. Sietsma, Diffusivity and viscosity during structural relaxation in metallic glasses, Mater. Sci. Eng. A 179–180 (1994) 86–90.
[29] Z.Q. Chen, L. Huang, F. Wang, P. Huang, T.J. Lu, K.W. Xu, Suppression of annealing-induced embrittlement in bulk metallic glass by surface crystalline coating, Mater. Des. 109 (2016) 179–185.
[30] Y.H. Liu, G. Wang, R.J. Wang, D.Q. Zhao, M.X. Pan, W.H. Wang, Super plastic bulk metallic glasses at room temperature, Science 315 (2007) 1385–1388.
[31] G. Daniel, V.H. Suong, W.T. Stephen, Composite Materials Design and Applications, Boca Raton, London, New York, Washington, 2003.
[32] Q. Zhou, J.Y. Xie, F. Wang, P. Huang, K.W. Xu, T.J. Lu, The mechanical behavior of nanoscale metallic multilayers: a survey, Acta Mech. Sin. 31 (2015) 319–337.
[33] T.G. Nieh, Y. Yang, J. Lu, C.T. Liu, Effect of surface modifications on shear banding and plasticity in metallic glasses: an overview, Prog. Nat. Sci. Mater. 22 (2012) 355–363.
[34] R. Raghavan, R. Ayer, H.W. Jin, C.N. Marzinsky, U. Ramamurty, Effect of shot peening on the fatigue life of a Zr-based bulk metallic glass, Scr. Mater. 59 (2008) 167–170.
[35] Y. Zhang, W.H. Wang, A.L. Greer, Making metallic glasses plastic by control of residual stress, Nat. Mater. 5 (2006) 857–860.
[36] W. Chen, K.C. Chan, S.H. Chen, S.F. Guo, W.H. Li, G. Wang, Plasticity enhancement of a Zr-based bulk metallic glass by an electroplated Cu/Ni bilayered coating, Mater. Sci. Eng. A 552 (2012) 199–203.
[37] J.L.G. Ravichandran, Pressure-dependent flow behavior of $Zr_{41.2}Ti_13.8Cu_{12.5}Ni_{10Be22}.5$ bulk metallic glass, J. Mater. Res. 18 (2003) 2039–2049.
[38] Q. Wei, K.T. Ramesh, B.E. Schuster, L.J. Kecskes, R.J. Dowding, Nanoengineering opens a new era for tungsten as well, JOM 58 (2006) 40–44.
[39] Z.W. Zhu, H.F. Zhang, W.S. Sun, B.Z. Ding, Z.Q. Hu, Processing of bulk metallic glasses with high strength and large compressive plasticity in $Cu_{50Zr}50$, Scr. Mater. 54 (2006) 1145–1149.
[40] W. Li, Y. Gao, H. Bei, On the correlation between microscopic structural heterogeneity and embrittlement behavior in metallic glasses, Sci. Rep. 5 (2015) 14786.
[41] N. Van Steenberge, A. Concustell, J. Sort, J. Das, N. Mattern, A. Gebert, S. Suriñach, J. Eckert, M.D. Baró, Microstructural inhomogeneities introduced in a Zr-based bulk metallic glass upon low-temperature annealing, Mater. Sci. Eng. A 491 (2008) 124–130.
[42] M. Wakeda, Y. Shibutani, S. Ogata, J. Park, Relationship between local geometrical factors and mechanical properties for Cu–Zr amorphous alloys, Intermetallics 15 (2007) 139–144.